HHS Public Access

Author manuscript

Oncogene. Author manuscript; available in PMC 2013 August 21.

Published in final edited form as:

Oncogene. 2013 February 21; 32(8): 1010–1017. doi:10.1038/onc.2012.124.

PKCα phosphorylation of RhoGDI2 at Ser 31 disrupts interactions with Rac1 and decreases GDI activity

Erin M. Griner[1], **Mair E.A. Churchill**[2,3], **David L. Brautigan**[1], and **Dan Theodorescu**[2,3,*]

[1]Center for Cell Signaling and Department of Microbiology, Immunology and Cancer Biology University of Virginia, Charlottesville, VA, USA, 22908

[2]Department of Pharmacology, University of Colorado, Aurora, Colorado, USA, 80045

[3]University of Colorado Comprehensive Cancer Center, Aurora, Colorado, USA, 80045

Abstract

Rho family GTPases control a diverse range of cellular processes, and their deregulation has been implicated in human cancer. Guanine nucleotide dissociation inhibitors (GDIs) bind and sequester GTPases in the cytosol, restricting their actions. RhoGDI2 is a member of the GDI family that acts as a metastasis suppressor in a variety of cancer types; however, very little is known about the regulation and function of this protein. Here we present a mechanism for inactivation of RhoGDI2 via PKC phosphorylation of Ser 31 in a region that contacts GTPases. In cells, RhoGDI2 becomes rapidly phosphorylated at Ser 31 in response to phorbol 12-myristate 13-acetate stimulation. Based on the effects of pharmacological inhibitors and knockdown by siRNA, we determine that conventional type PKCα is responsible for this phosphorylation. Phospho-mimetic S31E-RhoGDI2 exhibits reduced binding to Rac1 relative to wild type, with a concomitant failure to reduce levels of activated endogenous Rac1 or remove Rac1 from membranes. These results reveal a mechanism of down-regulation of RhoGDI2 activity through PKC mediated phosphorylation of Ser 31. We hypothesize that this mechanism may serve to neutralize RhoGDI2 function in tumors that express RhoGDI2 and active PKCα.

Keywords

RhoGDI2; phosphorylation; GTPase; PKCα

INTRODUCTION

The Rho family of small GTPases, the best studied of which are Rho, Rac and Cdc42, play important regulatory roles in diverse cell functions such as motility, growth, and differentiation (1, 2). Inappropriate activation of Rho GTPases is implicated in uncontrolled

*Corresponding author: Dan Theodorescu, Departments of Surgery and Pharmacology and University of Colorado Comprehensive Cancer Center, Aurora, CO 80045, Tel: 303-724-7135, Fax: 303-724-3162, dan.theodorescu@ucdenver.edu.

CONFLICT OF INTEREST

The authors declare no conflict of interest.

cell growth, invasion and metastasis of many types of cancers (3–5). GTPases cycle between active, guanosine triphosphate (GTP) bound states and inactive, guanosine diphosphate (GDP) bound states, and the rate at which this cycle occurs is regulated by three classes of proteins: guanine nucleotide exchange factors (GEFs), GTPase activating proteins (GAPs), and guanine nucleotide dissociation inhibitors (GDIs) (6).

The RhoGDI family consists of three members (RhoGDI1, 2 and 3) that bind to Rho family GTPases, extract them from membranes, and sequester them in the cytosol, effectively maintaining them in an inactive state and disallowing effector binding (7). GDIs are further thought to stabilize GTPases in the cytosol, enabling them to evade degradation (8). Importantly, both RhoGDI1 and RhoGDI2 (also called LyGDI or D4GDI) have been linked to tumorigenesis and metastasis, although their precise roles in cancer vary with tumor type (9). For instance, RhoGDI2 expression is downregulated in several cancer types including bladder, lung and lymphoma (10–14), but is upregulated in prostate and gastric cancer (15, 16). Further, although they share sequence similarity, RhoGDI1 and RhoGDI2 appear to carry out different functions within the same tumor type. For example, RhoGDI2 is a potent metastasis suppressor in bladder while RhoGDI1 only weakly suppresses metastasis (17), underscoring functional differences between RhoGDI1 and RhoGDI2.

Given the role of GDIs in cancer progression, it is important to understand how these proteins are regulated in both a normal and cancer setting. Recent identification of Tyr 153 as a Src phosphorylation site on RhoGDI2 that enhances RhoGDI2 metastasis suppressor function in experimental lung metastasis assays of bladder cancer cells highlighted that phosphorylation of RhoGDI2 can modulate its metastasis suppressor function (18). Given this, we sought to identify additional post-translational modifications of RhoGDI2, and determine whether they alter GDI function. Here we identify Ser31 in RhoGDI2 as a site that, when phosphorylated by PKCα, inhibits RhoGDI2 function by reducing its binding to Rac1, which leads to increased Rac1 activation and decreased cytosolic sequestration.

RESULTS

RhoGDI2 is phosphorylated in cells in response to phorbol ester treatment

Previous studies showed by ^{32}P labeling that RhoGDI2 was phosphorylated in response to phorbol-12-myristate-13-acetate (PMA) treatment of U937 human myelomonocytic cells and Jurkat cells (19, 20), although no further analysis was performed. Because PMA is a potent activator of the Protein Kinase C (PKC) family of enzymes, we decided to test whether RhoGDI2 was phosphorylated by PKC. We utilized a phospho-specific PKC substrate antibody that recognizes phosphorylated proteins with a PKC consensus sequence ([R/K]XpS[Hyd][R/K]) to assess RhoGDI2 phosphorylation in cells. We found that FLAG-RhoGDI2 expressed in 293T cells was phosphorylated at a PKC site in response to PMA in a dose-dependent manner (Fig. 1A). Phosphorylation was abolished by pre-treatment of the cells with the pan-PKC inhibitor GF 109203X (Fig. 1A), reinforcing that this is a PKC-mediated phosphorylation. PMA induced phosphorylation of RhoGDI2 was maximal within 10 minutes and persisted at an elevated level for as long as an hour (Fig. 1B). To assess the maximum extent of this phosphorylation, we determined by immunoblotting the fraction of total FLAG-RhoGDI2 that exhibited reduced electrophoretic mobility following PMA

treatment (Fig. 1C). We found that PMA induced phosphorylation of approximately 45% of the RhoGDI2 protein, indicating efficient and extensive phosphorylation in response to PMA. In order to demonstrate that endogenous RhoGDI2 also was phosphorylated in response to PMA, endogenous RhoGDI2 was immunoprecipitated from Jurkat cell extracts and probed for phosphorylation by immunoblotting using the phospho-PKC substrate antibody. While untreated Jurkat cells had no detectable RhoGDI2 phosphorylation, PMA treatment induced PKC-mediated phosphorylation of endogenous RhoGDI2 (Fig. 1D).

Serine 31 is the major site of PMA mediated phosphorylation

We employed mass spectrometry to identify sites of PMA induced phosphorylation. FLAG-RhoGDI2 was expressed in 293T cells treated with PMA, immunoprecipitated from cell extracts and isolated by SDS-PAGE. The band corresponding to FLAG-RhoGDI2 was visualized by Coomassie staining, excised, and digested. Peptides were analyzed using LC-MS/MS mass spectrometry. Sequence coverage spanned 92% of the protein (Fig. 2A), and two putative phospho-sites were identified, Ser20 and Ser31 (Fig. 2B). We made substitution mutants of both sites to alanine, S20A- and S31A-RhoGDI2, and assayed their phosphorylation by PKC in 293T cells in response to PMA treatment. Mutation of Ser 31 to Ala completely abolished PMA induced phosphorylation, while mutation of Ser 20 to Ala had no effect on phosphorylation (Fig. 2C), indicating that Ser 31 is the major site of PMA induced phosphorylation in RhoGDI2. The results with wild type and S31A-RhoGDI2 were replicated in UM-UC-3 bladder cancer cells (Fig. 2D).

PKCα phosphorylates RhoGDI2

We next wanted to identify the PKC isoform/s responsible for PMA induced Ser 31 phosphorylation in RhoGDI2. As a first approach, we pretreated 293T cells with either the pan-PKC inhibitor GF 109203X or the compound Gö 6976 that preferentially inhibits the conventional type PKC isoforms (PKCα, β, or γ). Both compounds abolished PMA induced phosphorylation of RhoGDI2 (Fig. 3A), indicating that one of the conventional PKCs may be responsible for RhoGDI2 phosphorylation. PKCγ expression is primarily but not exclusively restricted to neurons (21) and was not detected in 293T cells (22), so we concluded that either PKCα or PKCβ likely was responsible for RhoGDI2 phosphorylation. We used a SmartPool of siRNA oligos to knock down PKCα in UMUC3 bladder cells that were stably expressing FLAG-RhoGDI2. These cells were utilized because the effects of expressing RhoGDI2 in this cell type are well characterized (17, 18), and we have found they express high levels of PKCα relative to non-tumorigenic bladder cell lines (E.M. Griner and D. Theodorescu, unpublished observations). Knock down of PKCα was effective based on reduction in immunoblotting intensity and did not alter expression levels of PKCβ (Fig. 3B). Selective depletion of PKCα reduced PMA induced RhoGDI2 phosphorylation by over 70% (Fig. 3C) indicating that PKCα is the predominant PKC isoform involved in PMA mediated RhoGDI2 phosphorylation in these cells. We alternatively employed a single siRNA to knock down PKCα and observed a similar reduction in RhoGDI2 phosphorylation (Supplementary Fig. 1A).

To complement these data, we utilized a plasmid encoding myristoylated PKCα (Myr-PKCα) that is targeted to membranes as a highly active form of PKCα (23). Expression of

Myr-PKCα in 293T cells increased both basal and PMA stimulated levels of RhoGDI2 phosphorylation (Fig. 3D). Further, this enhanced phosphorylation was specific for Ser31, as the S31A-RhoGDI2 mutant was not phosphorylated in the presence of Myr-PKCα (Fig. 3D). Next, *in vitro* kinase assays were performed to determine if PKCα directly phosphorylated RhoGDI2. FLAG-RhoGDI2 was immunoprecipitated from untreated 293T cells, incubated with purified recombinant PKCα *in vitro*, and assessed for phosphorylation of Ser31 by Western blotting. Addition of recombinant PKCα to the assays led to robust phosphorylation of RhoGDI2, which was blocked entirely by the addition of the PKC inhibitor GF 109203X to the reaction (Fig. 3E). The S31A-RhoGDI2 mutant was not phosphorylated by PKCα *in vitro* (Fig. 3E) confirming that Ser31 was the site of PKCα mediated phosphorylation both *in vitro* and in cells. Together these data identified PKCα as the predominant PKC isoform responsible for PMA stimulated RhoGDI2 phosphorylation at Ser31.

Phospho-mimetic S31E-RhoGDI2 has reduced binding to Rac1

The major function of GDIs is to bind to small GTPases; therefore, we sought to determine the effect of Ser 31 phosphorylation on GTPase binding. As a first approach, we examined the three dimensional structure of RhoGDI2 bound to Rac2 (24). In this structure, residues 32–52 of the N-terminal portion of RhoGDI2 form a helix-loop-helix (helical hairpin) motif that is essential for Rac binding (Fig. 4A boxed region). This motif binds to the switch I and II regions of Rac and this interaction is further strengthened by contacts formed between residues 22–31 of RhoGDI2 and Rac (24). As seen in Fig. 4A, the hydroxyl oxygen of Ser 31 caps the first turn of the helical hairpin motif and forms two hydrogen bonds with Glu 34. Addition of a negatively charged phosphate group at Ser 31 would be expected to both eliminate stabilizing bonds and repel the negatively charged Glu 34 in the RhoGDI2 helical hairpin and ultimately lead to decreased binding affinity for Rac.

Given our structure-based predictions, we chose to assess the ability of RhoGDI2 Ser31 mutants to bind to Rac1, the major binding partner of RhoGDI2 (18). To do this we generated a phospho-mimetic mutant, S31E-RhoGDI2, and co-expressed it or wild type RhoGDI2 in 293T cells with HA-tagged Rac1. Proteins were immunoprecipitated using an anti-HA antibody and the amount of FLAG-RhoGDI2 that co-immunoprecipitated with Rac1 was analyzed by immunoblotting. While WT-RhoGDI2 effectively co-immunoprecipitated with Rac1, the levels of co-precipitated S31E-RhoGDI2 were lower (Fig. 4B), suggesting that the phospho-mimetic mutant has a reduced affinity for Rac1. Interestingly, the S31A-RhoGDI2 mutant also showed slightly reduced levels of immunoprecipitation with Rac1 that was significantly different from WT, but not reduced to the same extent as that for S31E-RhoGDI2. Loss of the polar hydroxyl group of Ser 31 by mutation to Ala would eliminate the two stabilizing bonds capping helix 1 and likely decrease the stability of the helical hairpin motif (Fig. 4A) at the Rac-RhoGDI2 interface. As a control, we performed the same set of experiments with S20A- and S20E-RhoGDI2. Neither the phospho-mimetic nor the non-phosphorylatable Ser 20 mutants showed significant changes in Rac1 binding relative to wild type (Supplementary Fig. 1B). We concluded that phosphorylation of RhoGDI2 at Ser 31 disrupts binding to Rac1.

From these data, we hypothesized that PMA treatment of cells would increase RhoGDI2 phosphorylation and therefore decrease the amount of RhoGDI2 bound to Rac1. Interestingly, we did not see a decrease in the amount of FLAG-RhoGDI2 that co-immunoprecipitated with HA-Rac1 after PMA treatment of cells (Fig. 4C). As controls, cells expressing RhoGDI2 were treated with PMA and RhoGDI2 immunoprecipitated using anti-FLAG antibody. While robust phosphorylation of the cellular pool of RhoGDI2 was seen in response to PMA treatment, no phosphorylation was detected in the RhoGDI2 that co-immunoprecipitated with Rac1, even when similar amounts of RhoGDI2 were compared in the Western blot (Fig. 4C). These results suggested that the non-phosphorylated form of RhoGDI2 preferentially binds to Rac1.

We immunoprecipitated endogenous RhoGDI2 from Jurkat cells with and without PMA stimulation. At this time point and concentration RhoGDI2 is effectively phosphorylated in response to PMA stimulation (Fig. 1D), We assayed by Western blot the amount of endogenous Rac1 co-immunoprecipitating with RhoGDI2, and found that PMA stimulation caused an approximately 30% decrease in Rac1 levels (Fig. 4D). These results show effects of PMA stimulation on Rac1 and RhoGDI2 binding, and agree with others who have previously reported that Rac1 is activated under these conditions (25).

S31E-RhoGDI2 has decreased activity as a Rac1 GDI protein

Knowing that S31E-RhoGDI2 has impaired ability to bind to Rac1, we surmised that S31E-RhoGDI2 also would be ineffective at reducing Rac1 activation. We assayed levels of activated endogenous Rac1 in 293T cells utilizing GST-Pak-Rac/Cdc42 (p21) binding domain (PBD) pull-down assays. Expression of WT-RhoGDI2 effectively reduced levels of activated Rac1 in cells, and the S31A-RhoGDI2 mutant behaved similarly to WT-RhoGDI2 (Fig. 5A). This is in keeping with the observation that under these conditions, RhoGDI2 exists largely in the unphosphorylated form that binds to Rac1 (Fig. 4C, **non-stimulated cells**). In contrast, S31E-RhoGDI2 had no effect on levels of active Rac1 compared to control cells, indicating that this mutant has diminished GDI function, most likely due to its reduced binding to Rac1 (Fig. 5A).

We also assayed for the ability of WT RhoGDI2 and the Ser 31 mutants to extract Rac1 from the membrane. While WT-RhoGDI2 effectively decreased levels of Rac1 found in the membrane fraction, the S31E-RhoGDI2 mutant failed to change Rac1 membrane distribution in comparison to control cells (Fig. 5B), further showing that S31E-RhoGDI2 has reduced binding to Rac1 and impaired GDI function. Interestingly, the S31A-RhoGDI2 mutant also did not significantly reduce Rac1 levels at the membrane, although it did trend towards reduced Rac1 in the membrane. Altogether these data suggest that RhoGDI2 phosphorylated at Ser 31 has impaired GDI function.

DISCUSSION

Here we identify Ser 31 as a phosphorylation site in RhoGDI2 that is induced by PMA treatment of cells, and we show that the conventional type PKCα is the predominant kinase involved in this phosphorylation. Comparison of the S31E-RhoGDI2 phospho-mimetic mutant to wild type RhoGDI2 revealed reduced Rac1 binding, an increase in Rac1

activation, and an inability to extract Rac1 from membranes. The results suggest PKC phosphorylation is a potential mechanism to inactivate the RhoGDI2 metastasis suppressor protein.

Structures of RhoGDI1 or RhoGDI2 bound to Rac identified two highly similar regions of RhoGDIs: a structurally stable C-terminal immunoglobulin like domain that binds the isoprenyl tail of GTPases, and a flexible N-terminal regulatory region consisting of a helical hairpin that binds to the switch I and II regions of Rac2 and inhibits GDP dissociation through stabilization of Mg^{+2} binding of switch I (24, 26, 27). The N-terminal region of the GDIs is essential for GTPase binding, as truncation of the first 41 residues disrupts protein structure and results in a loss of function (26). Ser 31 of RhoGDI2 is found in the N-terminal region of the protein and caps the first helix of the helical hairpin structure (24). The Ser 31 residue is conserved among all members of the RhoGDI family. Interestingly, the corresponding site in RhoGDI1 (Ser 34) has been identified as a substrate for conventional PKCs; however, Ser 34 RhoGDI1 phosphorylation led to a selective decrease in binding to RhoA, but not to Rac or Cdc42 (28). While these results suggest that both RhoGDI1 and RhoGDI2 are regulated by PKCs, phosphorylation does not produce identical effects on how different GDIs interact with Rho family GTPases. The mechanism through which this occurs is unclear, but may be related to the different binding affinities RhoGDI1 and RhoGDI2 have for GTPases.

Our analysis of the RhoGDI2-Rac2 complex indicates that the Ser 31 hydroxyl group of RhoGDI2 is involved in two hydrogen bonds with Glu 34 that form a cap at the N-terminus of helix 1 (Fig. 4A). Because Ser 31 interacts with an acidic side chain, phosphorylation or substitution of Ser 31 with an acidic residue would cause electrostatic repulsion in addition to the loss of the stabilizing hydrogen bonds, and would be expected to disrupt RhoGDI2 structure and decrease its interactions with Rac. Furthermore, the residues surrounding Ser 31 make important contacts with Rac (24, 26), and it is foreseeable that phosphorylation of Ser31 could also disrupt these contacts and further interfere with GTPase binding. NMR studies of RhoGDI1 or RhoGDI2 showed that the N-terminal 60 residues of the proteins were flexible and disordered when free in solution, but became ordered and formed a helical hairpin structure upon addition of Rac (26, 27). This model suggests that the N-terminal region of RhoGDI2 exists in an equilibrium between a disordered state and an ordered state, and that binding of RhoGDIs to a GTPase stabilizes the ordered state and the helical hairpin structure that is essential for GTPase binding (26). From this model and our data presented here, we propose that phosphorylation of Ser 31 drives RhoGDI2 towards an unstructured form and prevents binding of RhoGDI2 to a GTPase.

While results obtained with the S31A-RhoGDI2 mutant vary, they are generally consistent with our structural analysis, and our proposed model of RhoGDI2 regulation by Ser 31 phosphorylation predicts the relative severity of the deficiencies caused by the amino acid substitutions or Ser 31 phosphorylation. Substitution of Ser 31 to Ala would eliminate the Ser 31 hydroxyl group hydrogen bonding with Glu 34 and would destabilize the protein and its interactions with Rac, although not to as great of an extent as phosphorylation of Ser 31 or mutation to an acidic residue. Thus, when viewed in terms of the equilibrium between an ordered and disordered state, mutation of Ser 31 to Ala would slightly shift the equilibrium

towards a more disordered state. This could explain the intermediate effect of S31A-RhoGDI2 on Rac1 binding (Fig. 4B). The effect of S31A-RhoGDI2 expression on Rac1 membrane distribution (Fig. 5B) also trends toward an intermediate effect between that of WT and S31E-RhoGDI2, although the effect of S31A-RhoGDI2 is not statistically significant from either WT or S31E-RhoGDI2 in this assay. On the other hand, Rac1 activation levels in the presence of S31A-RhoGDI2 are decreased to a similar extent as in samples expressing WT RhoGDI2 (Fig. 5A). While binding to Rac1 is decreased in the S31A-RhoGDI2 mutant, it does still bind to Rac1, and this seems to be enough to depress Rac1 activation levels. It stands to reason that the S31A-RhoGDI2 mutant would behave similarly to WT RhoGDI2 in Rac1 activation assays given that WT RhoGDI2 is largely unphosphorylated in unstimulated cells (See Fig. 4C, non-stimulated cells).

While several phosphorylation sites have been identified on RhoGDI1, only one other major phosphorylation site in RhoGDI2, Tyr 153, was identified prior to this work. Similar to Ser 31 phosphorylation, Src mediated phosphorylation of Tyr 153 results in decreased Rac1 binding and inability of RhoGDI2 to extract Rac1 from membranes. Because Tyr153 and Ser31 are in different structural domains of RhoGDI2, we imagine that even though phosphorylation reduces Rac1 binding in each case, it probably does so via different mechanisms. Interestingly, the phospho-mimetic Y153E-RhoGDI2 mutant has enhanced metastasis suppressor function in experimental lung metastasis assays of bladder cancer cells (18), indicating that Src phosphorylation at Tyr 153 is a means of positively regulating RhoGDI2 metastasis suppressor function in bladder. The mechanisms through which this occurs are unclear, but thought to be related to the redistribution of RhoGDI2 to membranes, occuring upon Tyr 153 phosphorylation. This is in contrast to Ser 31 phosphorylation, which does not appear to redistribute the protein as the majority of the S31E-RhoGDI2 phospho-mimetic mutant remains in the cytosol (Fig. 5B).

Given the effect of Tyr 153 on RhoGDI2 function, it is clear that phosphorylation of RhoGDI2 is an important mechanism to modulate its metastasis suppressor function. It is intriguing to speculate that PKCα mediated Ser 31 phosphorylation may also play a role in modulating RhoGDI2 metastasis suppression. Interestingly, PKCα protein levels have been shown to increase in bladder cancer with increasing tumor grade (29), and PKCα was found to be more active in transitional cell carcinomas of bladder when compared to adjacent normal tissue (30). Further, studies using pharmacological inihibition of conventional PKCs have shown that PKC α or β can enhance migration, invasion and cell growth of bladder cancer cells (31, 32), altogether suggesting that PKCα may be pro-tumorigenic, although extensive work remains to verify this. Thus, PKCα phosphorylation at Ser31 of RhoGDI2 may be an alternate means of modulating RhoGDI2 metastasis suppressor activity in tumor cells. Experiments to test this hypothesis will be the subject of future work.

MATERIALS AND METHODS

Cell Culture and Reagents

HEK 293T cells were maintained in DMEM with 10% FBS. Jurkat cells were maintained in RPMI supplemented with 10% heat inactivated FBS. UM-UC-3 cells were maintained in MEM supplemented with 10% FBS and 1mM sodium pyruvate. All cells were cultured in a

humidified 5% CO_2 atmosphere at 37°C. Phorbol 12-Myristate 13-Acetate (LC Laboratories), GF 109203X (Enzo), Gö 6976 (EMD) were purchased from the indicated suppliers.

Transfection, Immunoprecipitation, Mutagenesis and Rac-GTP Pull-down Assays

Transfections were carried out using Fugene HD (Roche) as per manufacturer's instructions and 24 h following transfection, cells were incubated for 16 h in the presence of 1% FBS unless otherwise indicated. For immunoprecipitations, cells were washed, then lysed in ice cold lysis buffer (20 mM Tris, pH 7.4, 150 mM NaCl, 1mM EDTA, 1mM EGTA, 1% Triton X-100, 1 mM β-glycerophosphate) containing protease inhibitor cocktail and phosphatase inhibitor cocktail 3 (Sigma). Lysates were clarified by centrifugation at 13,000 g for 10 min and incubated with anti-FLAG M2 Agarose beads (Sigma) over night at 4°C. Beads were washed thrice with ice cold lysis buffer, boiled in sample buffer and eluted proteins were subjected to SDS-PAGE and Western blotting. Co-Immunoprecipitation was carried out with HEK 293T cells co-transfected with HA-Rac1 and FLAG-RhoGDI2 (WT or mutants) for 48 h. Cells growing in complete media were lysed as above. Extracts were incubated with anti-HA agarose (Sigma) over night at 4°C. Beads were washed thrice with cold lysis buffer, eluted with boiling sample buffer, and the proteins subjected to SDS-PAGE and Western blotting with anti-FLAG antibody (Sigma). For immunoprecipitations of endogenous RhoGDI2, Jurkat cells were lysed in lysis buffer (50 mM HEPES, 5 mM $MgCl_2$, 1 mM EGTA, 0.5% Triton X-100, pH 7.1), and lysates were clarified at 100K g for 30 minutes. Lysates were incubated with RhoGDI2 antibody conjugated to Protein A agarose beads for 2 h at 4°C, then washed thrice with lysis buffer. Mutagenesis was performed using the QuikChange site-directed mutagenesis kit (Stratagene) as per the manufacturer's instructions, using pFLAG-CMV-4-RhoGDI2 as template. Rac-GTP pull downs were performed on serum-depleted HEK 293T cells as described (33).

Western Blot Analysis, Antibodies and Subcellular Fractionation

Western blot images were acquired on an Odyssey Infrared Imaging System (Licor Biosciences) using anti-phospho-(Ser) PKC Substrate Antibody and anti-E-cadherin (Cell Signaling); anti-FLAG, anti-HA and anti-Vinculin (Sigma); anti-D4-GDI (RhoGDI2) (Spring Bioscience); anti-Rac1 (Upstate); anti-PKCα (Millipore); anti-PKCβ (Rockland) primary antibodies. Fractionation by ultracentrifugation was carried out as previously described (33).

Mass Spectrometry

FLAG-RhoGDI2 immunoprecipitated from PMA stimulated (1 μM, 10 min) HEK293T cells was subjected to SDS polyacrylamide gel electrophoresis, Coomassie stained, and excised from the gel. The gel piece was transferred to a siliconized tube and washed and destained in 200 μL 50% methanol overnight. The gel pieces were dehydrated in acetonitrile, rehydrated in 30 μL of 10 mM dithiothreitol in 0.1 M ammonium bicarbonate and reduced at room temperature for 0.5 h. The DTT solution was removed and the sample alkylated in 30 μL 50 mM iodoacetamide in 0.1 M ammonium bicarbonate at room temperature for 0.5 h. The reagent was removed and the gel pieces dehydrated in 100 μL acetonitrile. The acetonitrile was removed and the gel pieces rehydrated in 100 μL 0.1 M ammonium bicarbonate. The

pieces were dehydrated in 100 μL acetonitrile, the acetonitrile removed and the pieces completely dried by vacuum centrifugation. The gel pieces were rehydrated in 20 ng/μL trypsin in 50 mM ammonium bicarbonate on ice for 10 min. Any excess enzyme solution was removed and 20 μL 50 mM ammonium bicarbonate added. The sample was digested overnight at 37°C and the peptides formed extracted from the polyacrylamide in two 30 μL aliquots of 50% acetonitrile/5% formic acid. These extracts were combined and evaporated to 15 μL for MS analysis.

The LC-MS system consisted of a Finnigan LTQ-FT mass spectrometer system with a Protana nanospray ion source interfaced to a self-packed 8 cm × 75 μm id Phenomenex Jupiter 10 μm C18 reversed-phase capillary column. 0.5–5 μL volumes of the extract were injected and the peptides eluted from the column by an acetonitrile/0.1 M acetic acid gradient at a flow rate of 0.25 μL/min. The nanospray ion source was operated at 2.8 kV. The digest was analyzed using the double play capability of the instrument acquiring full scan mass spectra to determine peptide molecular weights and product ion spectra to determine amino acid sequence in sequential scans. This mode of analysis produces approximately 3000 CAD spectra of ions ranging in abundance over several orders of magnitude. Not all CAD spectra are derived from peptides. The data were analyzed by database searching using the Sequest search algorithm against RhoGDI2. Potentially modified peptides were confirmed manually.

RNA Interference

Double-stranded RNAs (100nM) were transfected into UM-UC-3 cells expressing FLAG-RhoGDI2 using Oligofectamine (Invitrogen). After 24 h, cells were serum starved for 16 h, pretreated with calyculin A (25 nM, 30 min), then treated with PMA (1μM, 10 min) and lysed. FLAG-RhoGDI2 was immunoprecipitated as described above and assessed for phosphorylation. RNA duplexes used were: ON-TARGET plus Smart Pool Catalog # L-003523-00(Dharmacon), Non-Targeting Control (CATCGCTGTAGCATCGTCT), or PKCα (AATCCTTGTCCAAGGAGGCTG).

In vitro Kinase assay

RhoGDI2 immunoprecipitated from untreated HEK293T cells was incubated for 15 min at 30°C with recombinant human PKCα (50 ng) (Calbiochem) in 20 mM HEPES, 10 mM $MgCl_2$, 100 μM $CaCl_2$, 20 μg of phosphatidylserine vesicles, 100 nM PMA, and 10 μM ATP. GF109203X was added at 5 μM.

Structural Analysis

Visual inspection and measurement of structural parameters were performed using PyMol (DeLano, W. L. 2008. The PyMOL Molecular Graphics System. DeLano Scientific, Palo Alto, CA.). Fig. 4A was generated from PDB entry 1SD6 (24) using PyMol and Photoshop (Adobe).

Statistical Analysis

Images were analyzed using Image J software (NIH). Data are expressed as mean ± S.E. and analyzed using a Student's t test. A p value of <0.05 was considered statistically significant.

All results shown are representative of three independent experiments unless otherwise indicated.

Supplementary Material

Refer to Web version on PubMed Central for supplementary material.

Acknowledgments

Myr-PKCα was a generous gift of Dr. Marcelo G. Kazanietz (University of Pennsylvania). This work was supported by National Institutes of Health grant CA143971 to D.T. E.M.G. was supported by the Paul Mellon Urologic Cancer Institute (Charlottesville, VA).

References

1. Heasman SJ, Ridley AJ. Mammalian Rho GTPases: new insights into their functions from in vivo studies. Nature Reviews Molecular Cell Biology. 2008 Sep; 9(9):690–701. [PubMed: 18719708]
2. Jaffe AB, Hall A. Rho GTPases: Biochemistry and biology. Annual Review of Cell and Developmental Biology. 2005:247–69.
3. Kamai T, Tsujii T, Arai K, Takagi K, Asami H, Ito Y, et al. Significant association of Rho/ROCK pathway with invasion and metastasis of bladder cancer. Clinical Cancer Research. 2003 Jul; 9(7): 2632–41. [PubMed: 12855641]
4. Pervaiz S, Cao J, Chao OSP, Chin YY, Clement MV. Activation of the RacGTPase inhibits apoptosis in human tumor cells. Oncogene. 2001 Sep 27; 20(43):6263–8. [PubMed: 11593437]
5. Vega FM, Ridley AJ. Rho GTPases in cancer cell biology. Febs Letters. 2008 Jun 18; 582(14): 2093–101. [PubMed: 18460342]
6. VanAelst L, DsouzaSchorey C. Rho GTPases and signaling networks. Genes & Development. 1997 Sep 15; 11(18):2295–322. [PubMed: 9308960]
7. DerMardirossian C, Bokoch GM. GDIs: central regulatory molecules in Rho GTPase activation. Trends in Cell Biology. 2005 Jul; 15(7):356–63. [PubMed: 15921909]
8. Boulter E, Garcia-Mata R, Guilluy C, Dubash A, Rossi G, Brennwald PJ, et al. Regulation of Rho GTPase crosstalk, degradation and activity by RhoGDI1. Nature Cell Biology. 2010 May; 12(5): 477–U136. [PubMed: 20400958]
9. Harding MA, Theodorescu D. RhoGDI signaling provides targets for cancer therapy. European Journal of Cancer. 2010 May; 46(7):1252–9. [PubMed: 20347589]
10. Gildea JJ, Seraj MJ, Oxford G, Harding MA, Hampton GM, Moskaluk CA, et al. RhoGD12 is an invasion and metastasis suppressor gene in human cancer. Cancer Research. 2002 Nov 15; 62(22): 6418–23. [PubMed: 12438227]
11. Lopez-Pedrera C, Villalba JM, Siendones E, Barbarroja N, Gomez-Diaz C, Rodriguez-Ariza A, et al. Proteomic analysis of acute myeloid leukemia: Identification of potential early biomarkers and therapeutic targets. Proteomics. 2006 Apr; 6(Suppl 1):S293–9. [PubMed: 16521150]
12. Ma L, Xu G, Sotnikova A, Szczepanowski M, Giefing M, Krause K, et al. Loss of expression of LyGDI (ARHGDIB), a rho GDP-dissociation inhibitor, in Hodgkin lymphoma. British Journal of Haematology. 2007 Oct; 139(2):217–23. [PubMed: 17897297]
13. Niu H, Li H, Xu C, He P. Expression profile of RhoGDI2 in lung cancers and role of RhoGDI2 in lung cancer metastasis. Oncology Reports. 2010 Aug; 24(2):465–71. [PubMed: 20596634]
14. Theodorescu D, Sapinoso LM, Conaway MR, Oxford G, Hampton GM, Frierson HF. Reduced expression of metastasis suppressor RhoGD12 is associated with decreased survival for patients with bladder cancer. Clinical Cancer Research. 2004 Jun 1; 10(11):3800–6. [PubMed: 15173088]
15. Abiatari I, DeOliveira T, Kerkadze V, Schwager C, Esposito I, Giese NA, et al. Consensus transcriptome signature of perineural invasion in pancreatic carcinoma. Molecular Cancer Therapeutics. 2009 Jun; 8(6):1494–504. [PubMed: 19509238]

16. Cho HJ, Baek KE, Park S-M, Kim I-K, Choi Y-L, Cho H-J, et al. RhoGDI2 Expression Is Associated with Tumor Growth and Malignant Progression of Gastric Cancer. Clinical Cancer Research. 2009 Apr 15; 15(8):2612–9. [PubMed: 19351766]
17. Moissoglu K, McRoberts KS, Meier JA, Theodorescu D, Schwartz MA. Rho GDP Dissociation Inhibitor 2 Suppresses Metastasis via Unconventional Regulation of RhoGTPases. Cancer Research. 2009 Apr 1; 69(7):2838–44. [PubMed: 19276387]
18. Wu Y, Moissogiu K, Wang H, Wang X, Frierson HF, Schwartz MA, et al. Src phosphorylation of RhoGDI2 regulates its metastasis suppressor function. Proceedings of the National Academy of Sciences of the United States of America. 2009 Apr 7; 106(14):5807–12. [PubMed: 19321744]
19. Gorvel JP, Chang TC, Boretto J, Azuma T, Chavrier P. Differential properties of D4/LyGDI versus RhoGDI: phosphorylation and rho GTPase selectivity. Febs Letters. 1998 Jan 30; 422(2):269–73. [PubMed: 9490022]
20. Scherle P, Behrens T, Staudt LM. LY-GDI, A GDP-Dissociation Inhibitor of the RhoA GTP-Binding Protein, is Expressed Preferentially in Lymphocytes. Proceedings of the National Academy of Sciences of the United States of America. 1993 Aug 15; 90(16):7568–72. [PubMed: 8356058]
21. Saito N, Shirai Y. Protein kinase C gamma (PKC gamma): Function of neuron specific isotype. Journal of Biochemistry. 2002 Nov; 132(5):683–7. [PubMed: 12417016]
22. Rex EB, Rankin ML, Yang Y, Lu Q, Gerfen CR, Jose PA, et al. Identification of RanBP 9/10 as Interacting Partners for Protein Kinase C (PKC) gamma/delta and the D(1) Dopamine Receptor: Regulation of PKC-Mediated Receptor Phosphorylation. Molecular Pharmacology. 2010 Jul; 78(1):69–80. [PubMed: 20395553]
23. Rabinovitz I, Toker A, Mercurio AM. Protein kinase C-dependent mobilization of the alpha 6 beta 4 integrin from hemidesmosomes and its association with actin-rich cell protrusions drive the chemotactic migration of carcinoma cells. Journal of Cell Biology. 1999 Sep 6; 146(5):1147–59. [PubMed: 10477766]
24. Scheffzek K, Stephan I, Jensen ON, Illenberger D, Gierschik P. The Rac-RhoGDI complex and the structural basis for the regulation of Rho proteins by RhoGDI. Nature Structural Biology. 2000 Feb; 7(2):122–6. [PubMed: 10655614]
25. Siliceo M, Garcia-Bernal D, Carrasco S, Diaz-Flores E, Leskow FC, Teixido J, et al. beta 2-chimaerin provides a diacylglycerol-dependent mechanism for regulation of adhesion and chemotaxis of T cells. J Cell Sci [Article]. 2006 Jan; 119(1):141–52.
26. Golovanov AP, Chuang TH, DerMardirossian C, Barsukov I, Hawkins D, Badii R, et al. Structure-activity relationships in flexible protein domains: Regulation of rho GTPases by RhoGDI and D4 GDI. Journal of Molecular Biology. 2001 Jan 5; 305(1):121–35. [PubMed: 11114252]
27. Keep NH, Barnes M, Barsukov I, Badii R, Lian LY, Segal AW, et al. A modulator of rho family G proteins, rhoGDI, binds these G proteins via an immunoglobulin-like domain and a flexible N-terminal arm. Structure. 1997 May 15; 5(5):623–33. [PubMed: 9195882]
28. Dovas A, Choi Y, Yoneda A, Multhaupt HAB, Kwon S-H, Kang D, et al. Serine 34 Phosphorylation of Rho Guanine Dissociation Inhibitor (RhoGDI alpha) Links Signaling from Conventional Protein Kinase C to RhoGTPase in Cell Adhesion. Journal of Biological Chemistry. 2010 Jul 23; 285(30):23294–306.
29. Koren R, Langzam L, Paz A, Livne PM, Gal R, Sampson SR. Protein kinase C (PKC) isoenzymes immunohistochemistry in lymph node revealing solution-fixed, paraffin-embedded bladder tumors. Applied Immunohistochemistry & Molecular Morphology. 2000 Jun; 8(2):166–71. [PubMed: 10937066]
30. Aaltonen V, Koivunen J, Laato M, Peltonen J. Heterogeneity of cellular proliferation within transitional cell carcinoma: Correlation of protein kinase C alpha/betal expression and activity. Journal of Histochemistry & Cytochemistry. 2006 Jul; 54(7):795–806. [PubMed: 16517978]
31. Aaltonen V, Peltonen J. PKC alpha/beta I Inhibitor Go6976 Induces Dephosphorylation of Constitutively Hyperphosphorylated Rb and G(1) Arrest in T24 Cells. Anticancer Research. 2010 Oct; 30(10):3995–9. [PubMed: 21036713]

32. Koivunen J, Aaltonen V, Koskela S, Lehenkari P, Laato M, Peltonen J. Protein kinase C alpha/beta inhibitor Go6976 promotes formation of cell junctions and inhibits invasion of urinary bladder carcinoma cells. Cancer Research. 2004 Aug 15; 64(16):5693–701. [PubMed: 15313909]

33. Griner EM, Caino MC, Sosa MS, Colon-Gonzalez F, Chalmers MJ, Mischak H, et al. A Novel Cross-talk in Diacylglycerol Signaling: The Rac-GAP beta 2-chimaerin is Negatively Regulated by Protein Kinase C delta-Mediated Phosphorylation. Journal of Biological Chemistry. 2010 May 28; 285(22):16931–41. [PubMed: 20335173]

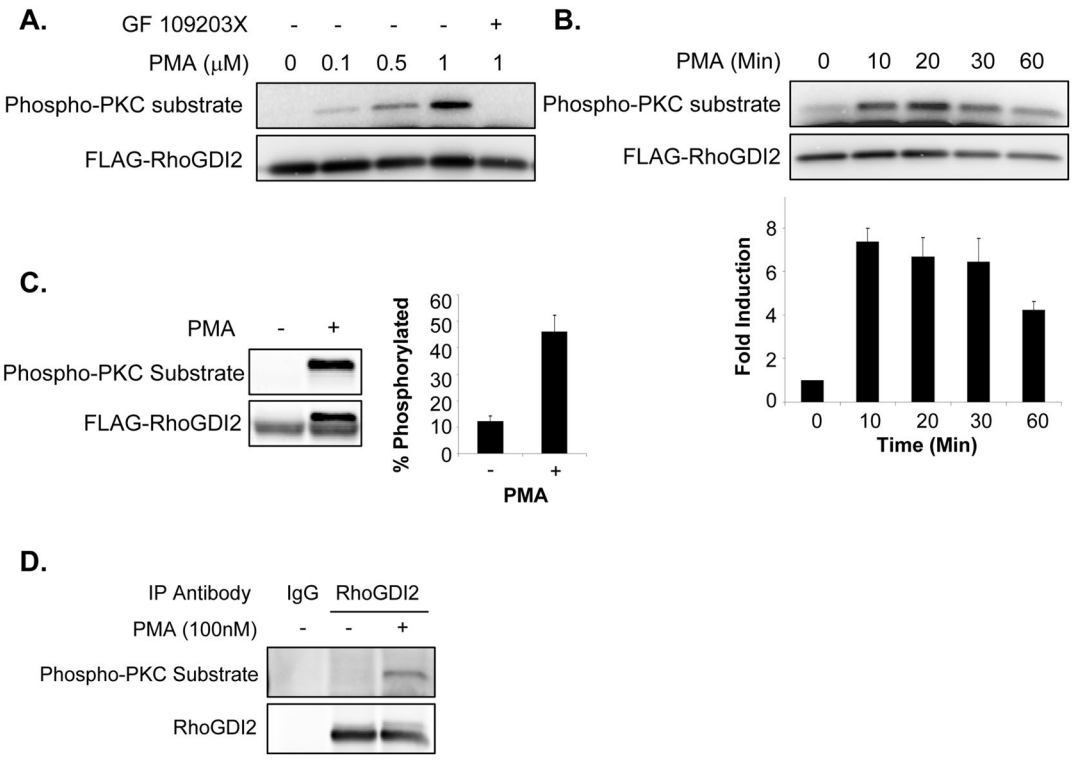

Figure 1. RhoGDI2 is phosphorylated in response to PMA stimulation

A. HEK 293T cells expressing FLAG-RhoGDI2 were treated with the indicated concentrations of PMA (10 min). GF 109203X was added as indicated (5 μM, 30 min). FLAG-RhoGDI2 was immunoprecipitated from lysates, and phosphorylation was assessed by Western blot using an anti-phospho PKC substrate antibody. Total levels of RhoGDI2 in immunoprecipitations (IPs) were assessed by anti-FLAG immunoblotting.

B. HEK 293T cells were treated with PMA (1 μM) for the indicated times and prepared as in 1A. Top, representative Western blots of IPs are shown. Bottom, results expressed as fold induction of phosphorylation relative to time 0 presented as mean ± S.E.

C. FLAG-RhoGDI2 IPs from PMA treated (1 μM, 10 min) HEK293T lysates were separated on 12.5% Criterion Tris-HCL polyacrylamide gels (BioRad), and a phosphorylation dependent gel shift was analyzed by Western blotting. Left, representative Western blots. Right, results expressed as percent phosphorylated protein in relation to total RhoGDI2 protein ([upper band intensity/(upper + lower band intensity)] × 100) presented as mean ± S.E.

D. Jurkat cells were treated with PMA (100 nM, 10 min) and the resulting lysates were immunoprecipitated using IgG control antibody or anti-RhoGDI2 antibody and Protein A agarose beads. Phosphorylation of endogenous RhoGDI2 was assessed by Western blot using an anti-phospho PKC substrate antibody and total RhoGDI2 was assessed using an anti-RhoGDI2 antibody.

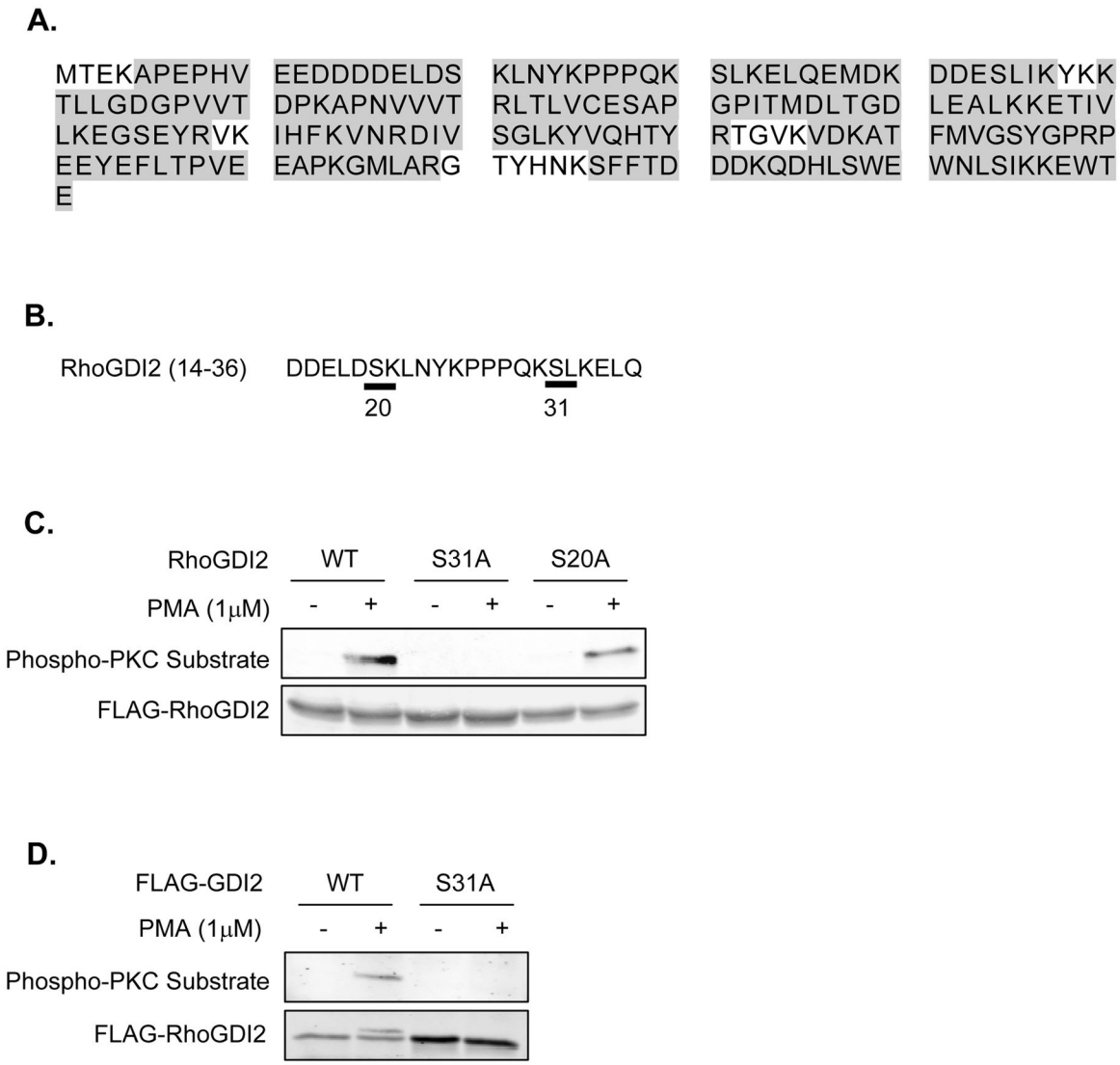

Figure 2. Serine 31 of RhoGDI2 is the major site of PMA induced phosphorylation

A. Coverage map of mass spectrometry analysis. Shaded areas represent regions of the protein that were identified by mass spec.

B. Sequence of residues 14–36 of human RhoGDI2. The putative phosphorylation sites (Ser 20 and Ser31) are underlined.

C. HEK 293T cells expressing WT-, S20A- or S31A –RhoGDI2 were treated with PMA (1 μM, 10 min), and phosphorylation of RhoGDI2 in anti-FLAG precipitates was assessed by Western blot using an anti-phospho PKC substrate antibody.

D. UM-UC-3 cells expressing FLAG-RhoGDI2 were treated with calyculin A (25 nM, 30 min), then treated with PMA (1 μM, 10 min) and lysed. Phosphorylation of RhoGDI2 in anti-FLAG IPs from lysates was assessed by Western blot using an anti-phospho PKC substrate antibody.

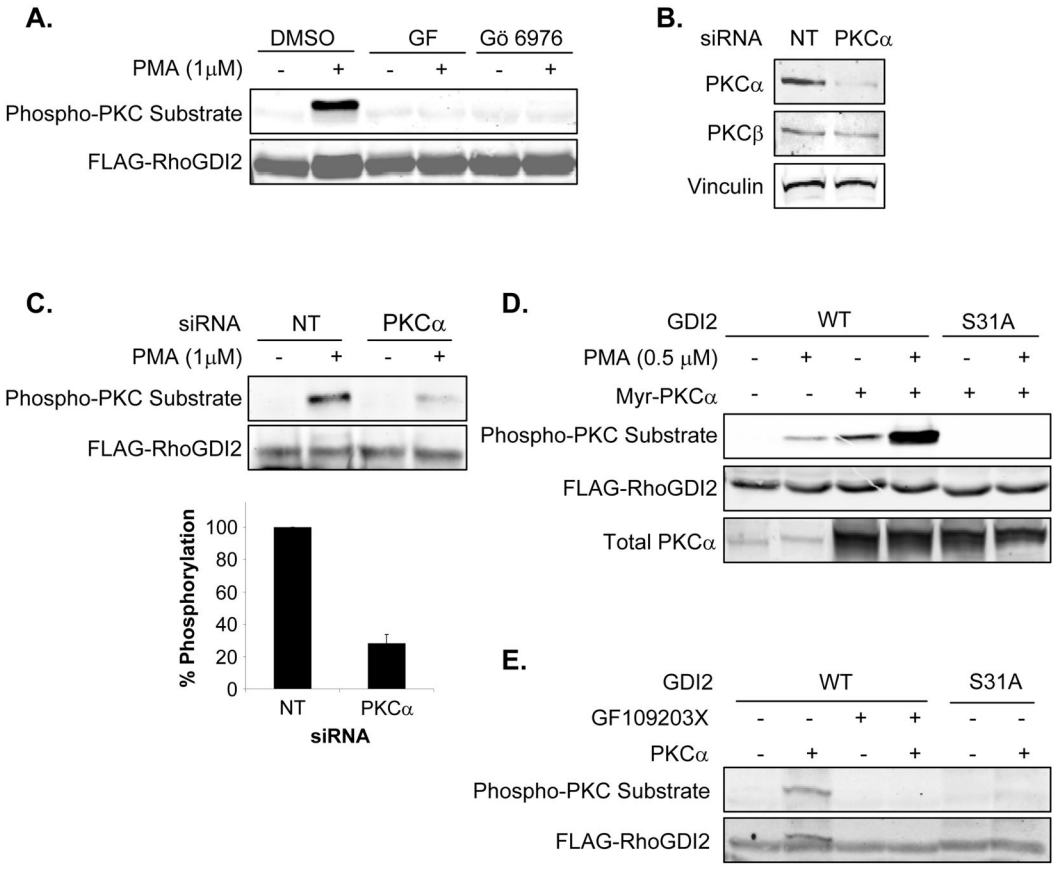

Figure 3. PKCα phosphorylates RhoGDI2 in response to PMA

A. HEK 293T cells expressing WT-RhoGDI2 were pretreated with the indicated PKC inhibitors (5 μM, 30 min), then treated with PMA (1 μM, 10 min). Phosphorylation of RhoGDI2 recovered in immunoprecipitates was assessed by Western blot using an anti-phospho-(Ser) PKC substrate antibody. GF, GF 109203X.

B. PKC expression in UM-UC-3 cells after PKCα knock down. NT, non-targeting control sequence.

C. UM-UC-3 cells expressing FLAG-RhoGDI2 were transfected with the indicated siRNA oligos. 48 h after knock down, cells were treated with calyculin A (25 nM, 30 min), then treated with PMA (1 μM, 10 min) and lysed. Phosphorylation of RhoGDI2 in anti-FLAG immunoprecipitates was assessed by Western blot using an anti-phospho PKC substrate antibody. Top, representative Western blots. Bottom, results expressed as percent phosphorylated protein in relation to NT (+ PMA) presented as mean ± S.E. (n=4).

D. HEK 293T cells expressing RhoGDI2 and Myr-PKCα were treated with PMA (0.5 μM, 10 min), and phosphorylation of RhoGDI2 in IPs was assessed by Western blot using an anti-phospho PKC substrate antibody. PKCα expression was determined by Western blotting of total protein.

E. *in vitro* phosphorylation of RhoGDI2 by recombinant PKCα was measured by Western blot.

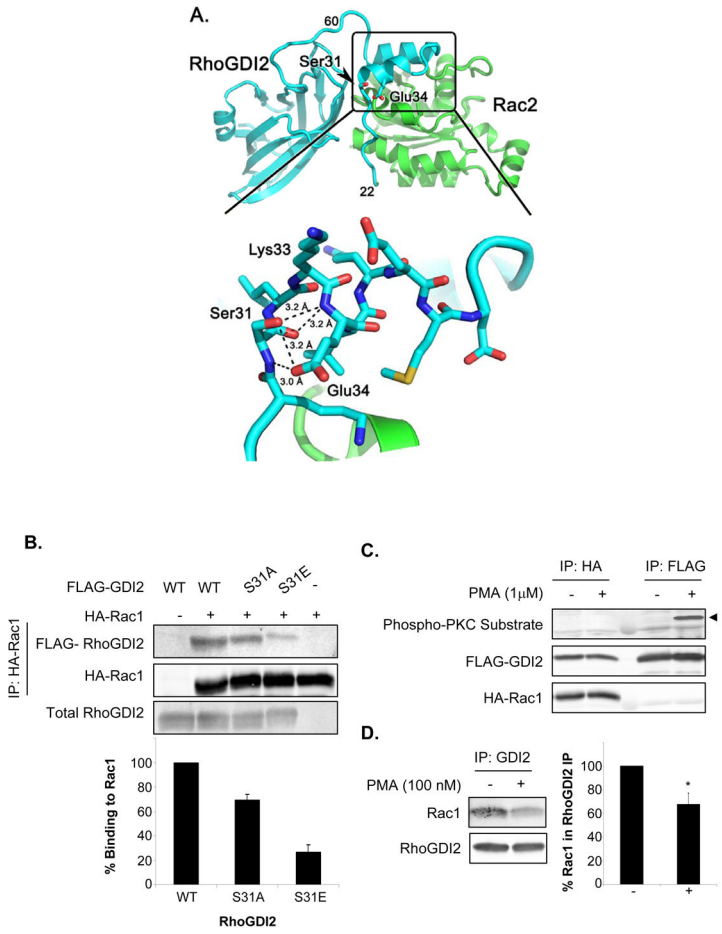

Figure 4. Importance of Ser 31 in the RhoGDI2-Rac2 complex

A. Ribbon diagram showing the interaction between RhoGDI2 (cyan) and Rac2 (green) in the crystal structure of the RhoGDI2-Rac2 complex (PDB ID 1DS6) (24). The site of Ser31 and Glu 34 and the RhoGDI2 helical hairpin motif are boxed. Box: Close of up view the interactions of RhoGDI2 Ser 31 and Glu 34. Ser 31 forms the N-terminal cap of helix 1 of the helical hairpin. Atoms are colored blue for nitrogen, red for oxygen and yellow for sulfur. Inferred hydrogen bonds are shown as black dotted lines with distances indicated.

B. Extracts from HEK 293T cells co-transfected with HA-Rac1 and the indicated FLAG-RhoGDI2 constructs were immunoprecipitated with anti-HA agarose beads and the amount of FLAG-RhoGDI2 co-precipitating was assayed by Western blot. Top, representative Western blots. Bottom, results expressed as percent binding to Rac1 relative to WT-RhoGDI2 presented as the mean ± S.E. ($n \geq 4$). *, $p<0.05$. ***, $p<0.001$.

C. Phosphorylation status of RhoGDI2 co-precipitated with Rac1 was measured using an anti-phospho PKC substrate antibody. As a control, anti-FLAG agarose beads were used to immunoprecipitate FLAG-RhoGDI2 to show that phosphorylated RhoGID2 was present. Arrowhead indicates FLAG-RhoGDI2.

D. Jurkat cells were treated with PMA (100 nM, 30 min) and the resulting lysates were immunoprecipitated using anti-RhoGDI2 antibody and Protein A agarose beads. Endogenous Rac1 co-immunoprecipitating with RhoGDI2 was assessed by Western blot.

Left, representative Western blots. Right, results expressed as percent Rac1 in IP relative to untreated samples presented as the mean ± S.E. (n = 3). *, $p<0.05$.

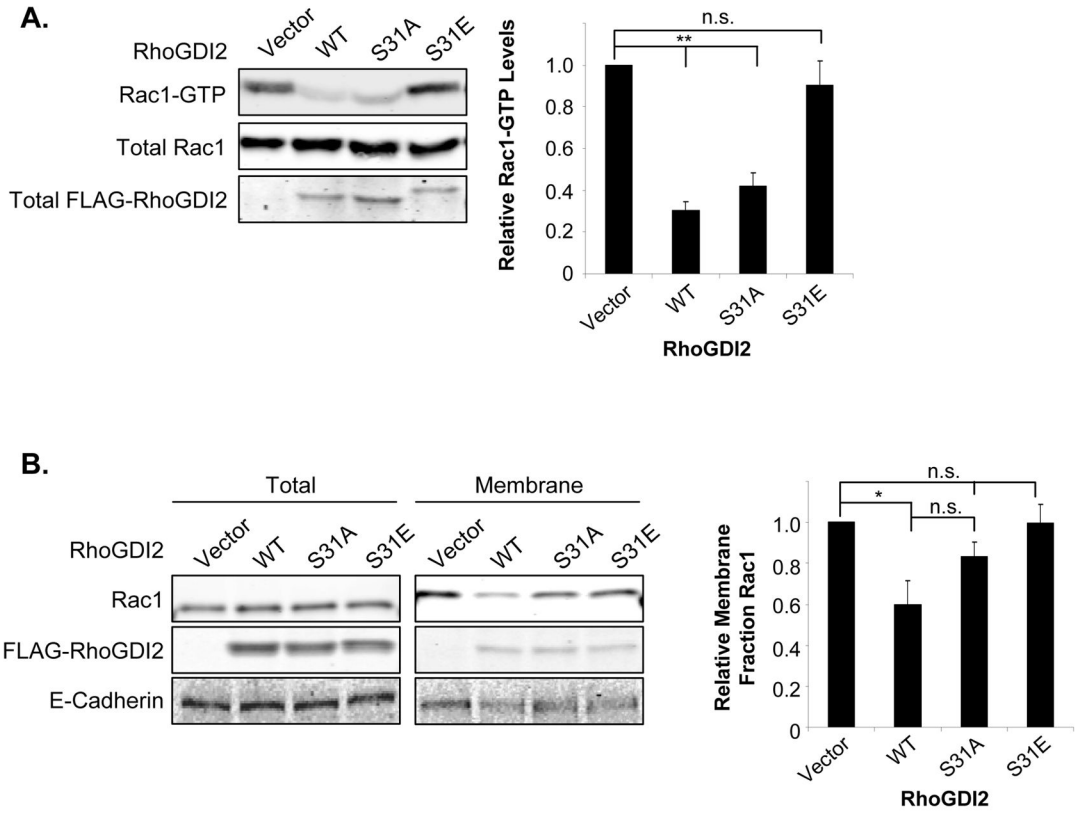

Figure 5. S31E-RhoGDI2 fails to reduce levels of activated Rac1 or relocalize Rac1 to the cytosol

A. Extracts from HEK 293T cells transfected with empty vector control, WT, S31A or S31E RhoGDI2 were assayed for levels of Rac1-GTP using pull-down assays. Left, representative Western blots. Right, results expressed as fold change relative to vector control presented as the mean ± S.E. ($n \geq 3$). **, $p<0.01$. n.s., not significant.

B. Extracts from HEK 293T cells treated as above were fractionated. Rac1 localization was assessed by Western blot. Left, representative Western blots. Right, results expressed as the fold change of RhoGDI2 localized in the insoluble fraction relative to vector control and normalized to total levels of Rac1 presented as the mean ± S.E. ($n = 4$). *, $p<0.05$. n.s., not significant.